HHS Public Access

Author manuscript

Alcohol. Author manuscript; available in PMC 2020 September 01.

Published in final edited form as:

Alcohol. 2019 September ; 79: 71–79. doi:10.1016/j.alcohol.2018.12.005.

Effect of Nanoformulated Copper/Zinc Superoxide Dismutase on Chronic Ethanol-Induced Alterations in Liver and Adipose Tissue

Gopalakrishnan Natarajan, PhD[1], **Curtis Perriotte-Olson, BS**[1], **Carol A Casey, PhD**[2,4], **Terrence M. Donohue Jr., PhD**[2,4], **Geoffrey A Talmon, MD**[3], **Edward N Harris, PhD**[5], **Alexander V Kabanov, PhD**[6], **Viswanathan Saraswathi, PhD**[1,4,*]

[1]Department of Internal Medicine, Divisions of Diabetes, Endocrinology, and Metabolism, University of Nebraska Medical Center

[2]Department of Internal Medicine, Divisions of Gastroenterology and Hepatology, University of Nebraska Medical Center

[3]Department of Pathology and Microbiology, University of Nebraska Medical Center

[4]VA Nebraska-Western Iowa Health Care System, Omaha, NE;

[5]Department of Biochemistry, University of Nebraska at Lincoln, Lincoln, NE;

[6]Division of Pharmacoengineering and Molecular Pharmaceutics, Eshelman School of Pharmacy, University of North Carolina at Chapel Hill, Chapel Hill, NC.

Abstract

Background.—We previously reported that nanoformulated copper/zinc superoxide dismutase (Nano) attenuates non-alcoholic fatty liver disease and adipose tissue (AT) inflammation in obese animals. Here, we sought to determine whether Nano treatment attenuates alcohol-associated liver disease (AALD) and AT inflammation in alcohol-fed mice.

Methods.—We pre-treated E-47 cells (HepG2 cells that over-express CYP2E1) with native- or nano-SOD for 6 h, followed by treatment with ethanol and/or linoleic acid (LA), a free fatty acid. For in vivo studies, male C57BL/6 mice were fed the Lieber-DeCarli control or ethanol liquid diet for 4 wk. The mice received Nano once every two days during the last 2 wk of ethanol feeding.

Results.—Our *in vitro* studies revealed that Nano pretreatment reduced LA+ethanol-induced oxidative stress in E-47 cells. Our *in vivo* experiments showed that ethanol-fed Nano-treated mice

[*]**Address correspondence to:** Viswanathan Saraswathi, Research Service, VA Nebraska Western Iowa Health Care System, Omaha, NE. Ph: 402-995-3033; Fax: 402-449-0604; s.viswanathan@unmc.edu.

Disclosure

AVK is the co-inventor of the nanozyme technology at UNMC (Patent number: WO2008141155A1). The technology and products have been exclusively out-licensed to NeuroNano Pharma, a start-up company located in Chapel Hill, NC. AVK is a co-founder, shareholder and director of this company. The other authors declare no conflict of interests.

had 22% lower hepatic triglyceride levels than mice fed ethanol alone. Nano-treated ethanol-fed mice also had 2-fold lower levels of *Cd68 and similarly-reduced levels of Ccl2* and *Mmp12* mRNAs, than in untreated ethanol-fed mice. We also noted that ethanol feeding caused a remarkable increase in hepatic and/or plasma MCP-1 and CCR2 protein which was blunted in ethanol+Nano-treated animals. The hepatic content of SREBP-1c a transcription factor that promotes lipogenesis, was higher in ethanol-fed mice than controls but was attenuated in ethanol +Nano-treated animals. Further, livers of ethanol+Nano-treated mice had significantly higher levels of phosphorylated AMPK than both control and ethanol-fed mice. In AT, the level of *Il6* mRNA a hepatoprotective cytokine, and that of *Arg1*, a marker of anti-inflammatory macrophages, were significantly increased in ethanol+Nano-treated mice compared with control mice.

Conclusion.—Our data indicate that Nano treatment attenuates ethanol-induced steatohepatitis and this effect is associated with an apparent activation of AMPK signaling. Our data also suggest that Nano induces Arg1 and IL-6 expression in AT suggesting anti-inflammatory effects in this tissue.

Keywords

Ethanol; SOD1; steatohepatitis; MCP1; AMPK

Introduction

Heavy alcohol drinking causes liver disease worldwide. Ethanol-induced oxidative stress initiates and propagates the pathogenesis of alcohol-associated liver disease (AALD). Although multiple mechanisms are involved in ethanol-induced oxidative stress, superoxide generated during ethanol metabolism plays an integral role in the pathogenesis of AALD (Boveris, Fraga, Varsavsky, & Koch, 1983; Ekstrom & Ingelman-Sundberg, 1989; Koch, Galeotti, Bartoli, & Boveris, 1991). Cytochrome P450-catalyzed ethanol metabolism is an important source of superoxide (Abdelmegeed et al., 2013; Wang, Wu, Yang, Gan, & Cederbaum, 2013) along with superoxide derived from mitochondrial respiration and impaired anti-oxidant defense [Reviewed in (Ekstrom & Ingelman-Sundberg, 1989)]. Evidence exists that ethanol feeding to rodents reduces the activity and/or levels of superoxide dismutase 1 (SOD1) (L. H. Chen, Xi, & Cohen, 1995; Polavarapu et al., 1998; M. Zhao, Matter, Laissue, & Zimmermann, 1996). Moreover, SOD1 knock-out mice exhibit worse ethanol-induced liver injury than wild type mice (Kessova, Ho, Thung, & Cederbaum, 2003) and this is associated with hepatic mitochondrial changes (Kessova & Cederbaum, 2007). It is also noteworthy that ethanol consumption causes mobilization of free fatty acids (FFAs) from adipose tissue to liver. Because CYP2E1 increased by ethanol consumption, has broad substrate specificity, and can oxidize free fatty acids (Laethem, Balazy, Falck, Laethem, & Koop, 1993; Sung, Kim, Park, Whang, & Lee, 2004), such reactions may also exacerbate hepatic oxidant stress during excessive ethanol consumption.

Although a link clearly exists between superoxide-induced oxidative stress and AALD, clinical studies have revealed no benefit of using antioxidant vitamins/supplements to treat patients with AALD. For example, in a study of patients with mild to moderate steatohepatitis, vitamin E therapy had no beneficial effect on liver function and mortality compared to placebo controls (Mezey, Potter, Rennie-Tankersley, Caballeria, & Pares, 2004).

In another study, the effect of an antioxidant regimen on alcoholic hepatitis was compared to antioxidants plus steroid therapy. No beneficial effect was seen in either of those groups compared to placebo controls (Stewart et al., 2007). These trials may have failed due to the incorrect choice of the antioxidants or poor delivery to tissues through oral intake. For example, vitamin E was used in most of the studies and it does not specifically scavenge superoxide (Gotoh & Niki, 1992). Moreover, vitamin E by itself can actually exert pro-oxidant effects under certain conditions (Ouchi, Ishikura, Konishi, Nagaoka, & Mukai, 2009; Stocker, 1999). While adenovirus-mediated expression of SOD1 alleviates early alcohol-induced liver injury in rats *in vivo* (Wheeler et al., 2001), numerous inherent properties of adenoviruses limit their clinical utility. One is that systemic administration of adenoviruses results in their acute accumulation in liver, causing hepatotoxicity. Furthermore, most humans have adenoviral neutralizing antibodies, which impede gene expression efficiency (Eto, Yoshioka, Mukai, Okada, & Nakagawa, 2008).

Compelling evidence suggests that encapsulating antioxidant enzymes in nanocarriers increases their half-lives and the functional efficacy of these enzymes *in vivo*. Because of their potential use in clinical settings, antioxidant enzymes remain attractive candidates for nanomedicine. Several types of nanoformulated SOD have been designed and studied for their efficacy in ameliorating various diseases including hypertension and lung injury (Rosenbaugh et al., 2010; White et al., 1989). We previously demonstrated that SOD1 encapsulated in poly-L-lysine and polyethylene glycol polymer, cross-linked with a reducible cross-linker (nanoSOD or Nano) effectively attenuated inflammation in adipose and vascular tissues as well as non-alcoholic fatty liver disease (NAFLD) in obese mice (Perriotte-Olson et al., 2016; Saraswathi et al., 2016). Here, we sought to determine whether Nano administration alleviates AALD and/or AT inflammation in mice.

Materials and Methods

NanoSOD preparation

Nano was synthesized, purified, and characterized as reported previously in detail (Manickam et al., 2012). Native bovine Cu/Zn SOD1 protein (Sigma-Aldrich) and polymer stock solutions were prepared in 10 mM HEPES containing 0.15 M NaCl (pH 7.4). The Cu/Zn SOD1 was mixed with poly L-lysine–polyethylene glycol copolymer (PLL–PEG). The Cu/Zn SOD-PLL-PEG complex was covalently stabilized using a reducible cross-linker, 3,3′-dithiobis[sulfosuccinimidylproprionate] (DTSSP; Thermo Fisher Scientific). The molar ratio of DTSSP/PLL50 was 0.5 and the crosslinked-nanoSOD was purified using size exclusion chromatography (small/intermediate scale) or centrifugal filtration (large scale). The size of Nano was estimated to be ~44 nm.

Animals and Diets

Nine-week old male C57BL/6J mice were purchased from Jackson Laboratories (Bar Harbor, ME). Mice were divided into two groups. The ethanol-fed group received 5% ethanol (v/v) *ad lib* for four weeks after a seven day ramp-up period from feeding control Lieber-DeCarli diet to the full-strength Lieber-DeCarli ethanol diet (1% v/v ethanol to a final concentration of 5% v/v ethanol) in the diet. Control mice were pair-fed with ethanol-

fed mice to maintain equal caloric consumption (Lieber & DeCarli, 1989). At the end of the second week, ethanol-fed mice and their pair-fed controls were each subdivided into 2 groups: 1) Control (Cont)-fed, 2) Cont+Nano treated, 3) ethanol-fed, and 4) ethanol+Nano-treated groups (n=8 per group). Mice in Cont+Nano and ethanol+Nano group received *i.p.* injections of Nano (diluted in 10 mM HEPES) at 1000 units/kg body weight once every 2 days for a period of 2 wk. The remaining control and ethanol-fed mice received IP injections of 10mM HEPES alone (vehicle). Thus, each mouse received a total of 8 injections during this period. A day after the final injection, all mice were euthanized after a 5 h fast. Liver and visceral adipose tissue (AT, the fat depot around the epididymis) and blood samples were collected. All procedures were approved by the Institutional Animal Care and Use Committee at the VA Nebraska-Western Iowa Health Care System.

Analysis of alanine aminotransferase and liver triglycerides

Plasma alanine aminotransferase (ALT), a marker of liver injury, was determined at the VA clinical laboratory using the Vitros Analyzer. Liver lipids were extracted according to the procedure of Folch *et al.* (Folch, Lees, & Sloane Stanley, 1957) with minor modifications. Aliquots of lipid extract were saponified to quantify the triglycerides using the triglyceride diagnostic kit (Thermo DMA kit, Thermo Electron Clinical Chemistry, Louisville, CO).

Multiplex analysis of plasma inflammatory markers

Plasma inflammatory markers such as MCP-1 and TNFα were measured by Luminex xMAP Technology using a Mouse Metabolic Magnetic Bead Panel (#MMHMAG-44K) following manufacturer's instructions. Briefly, 10 microliters of stored mouse serum in duplicate was mixed with sonicated beads for each marker along with matrix solution and assay buffer in each well of a 96-well plate and incubated overnight on an orbital shaker (110 rpm) at 4°C. The following day, detect ion antibodies were added and a magnetic plate holder was used to retain the beads during the washing steps. Quantification of beads with analyte standards and sample cargos were measured by a Luminex MAGPIX system. Quantification of each analyte was calculated using the manufacturer's software.

TBARS measurement

Lipid peroxidation was assessed by quantifying thiobarbituric acid-reactive substances (TBARS) following the procedure of Uchiyama & Mihara using malondialdehyde as a standard (Mihara & Uchiyama, 1978).

Histology

Liver tissues were fixed in 10% neutral buffered formalin. The tissues were embedded in paraffin and cut into 4-μm sections. Liver sections were stained with hematoxylin and eosin at the tissue sciences facility at the University of Nebraska Medical Center. These slides were reviewed by a board-certified anatomic pathologist to evaluate for significant alterations (i.e. steatosis, cell death, etc.)

For immunofluorescence, sections were de-paraffinized with three washes of xylene, followed by rehydration using 100%, 95%, 80%, and 50% ethanol, and rinsed in H_20 before antigen retrieval in 1x citrate buffer (Abcam). The sections were blocked in 5% serum, and

incubated with anti-MCP1 (Santa Cruz Biotechnology) or anti-CCR2 (Abcam), followed by IgG-conjugated Alexa Fluor 568 (Life Technologies). Autofluorescence was quenched using 0.1% Sudan Black B (Acros Organics) in 70% ethanol. The sections were mounted using ProLong gold antifade with DAPI (4',6-damidino-2-phenylindole) (Invitrogen). Images (20X) were taken using a Nikon Eclipse 80i inverted fluorescence microscope.

SOD1 activity

SOD1 activity was measured in liver samples using an SOD1 assay kit from Cayman Chemical. Briefly, liver homogenates were prepared as suggested by the manufacturers and the cytosolic fraction was used for the assay of SOD1 activity. SOD1 activity was expressed as units per mg protein.

RNA isolation and real-time PCR

Total RNA was extracted from liver and AT using the TRIzol reagent (Ambion, Life Technologies). RNA was quantified using a NanoDrop spectrophotometer and transcribed using 5x iScript Reverse Transcription Supermix (Bio-Rad). Real-time PCR was performed to determine the mRNA levels encoding proteins regulating inflammation and macrophage inflammatory phenotype. A delta delta CT method was used to calculate gene expression with values normalized to 18S ribosomal RNA.

Western Blot Analyses

Liver samples were homogenized in 20 mM Tris-HCl, 150 mM NaCl, 1 mM EDTA, 1 mM EGTA, 0.5% NP-40, 2.5 mM sodium pyrophosphate, 1 mM sodium orthovanadate, 1 mM β-glycerophosphate and a proteinase inhibitor cocktail (Roche Diagnostics). Proteins were solubilized in NuPAGE buffer, separated by SDS-PAGE, and immunoblotted onto a PVDF membrane. Proteins of interest were detected using antibodies against the following proteins from Santa Cruz Biotechnology: SOD1, Sterol regulatory element binding protein 1 (SREBP1). Antibodies against fatty acid synthase (FASN), phospho AMPKα (T172), total AMPKα, phospho ACC, total ACC, and β-actin were purchased from Cell Signaling Technology. CYP2E1 antibody was from Abcam and Alcohol dehydrogenase 1 (ADH1) antibody was originally obtained from Dr. Michael Felder at the University of South Carolina. GAPDH antibody was obtained from Millipore. Protein bands were visualized using the Odyssey System (LI-COR Biosciences) or enhanced chemiluminescence.

Cell Culture

E-47 cells that over-express CYP2E1 were obtained from Dr. Dahn Clemens at the University of Nebraska Medical Center. Cells were grown in DMEM supplemented with 10% FBS, and 1% penicillin and 1% streptomycin. G418 sulfate (400 μg/ml) was also added for negative selection.

Fatty Acid Treatment

The fatty acid treatment was carried out using media containing serum as the source of albumin as we described previously (Saraswathi & Hasty, 2009). Briefly, the fatty acids were first dissolved in ethanol and were added to DMEM containing 5% FBS before treating the

cells. This resulted in a fatty acid to albumin ratio of 4:1. We chose to use linoleic acid (LA) based on our previous reports that LA, a polyunsaturated fatty acid (PUFA), induces superoxide-mediated oxidative stress in endothelial cells (Saraswathi, Wu, Toborek, & Hennig, 2004; Viswanathan et al., 2003). Moreover, Kirpich *et al* have shown that a diet rich in unsaturated fatty acids, in particular, LA, exacerbated AALD in mice (Kirpich et al., 2012). Therefore, we examined the interaction between ethanol and LA in promoting oxidative stress in liver cells.

DCF Fluorescence

E47 cells were seeded into black walled 24-well plates and pretreated with native- or Nano-SOD for 6 h. The medium was changed and cells incubated overnight. The pretreated cells were then exposed to 50 mM ethanol and/or 120 μM linoleic acid (LA) in DMEM containing 5% FBS for 1.5 h. A stock of LA was dissolved in 100% ethanol and added to treatment medium containing 5% FBS as we previously reported (Saraswathi et al., 2004; Viswanathan et al., 2003). During the last 30 min of the treatment period, the cells were stained with 10 μM dichlorodihydrofluorescein (DCF) diacetate in the dark. Cells were rinsed in HEPES buffer and DCF fluorescence was read with a fluorescent plate reader at an excitation wavelength of 492 nm and emission wavelength of 517 nm as we reported earlier (Viswanathan et al., 2003).

Statistical Analyses

Data were analyzed by one-way ANOVA followed by Tukey's multiple comparison test using GraphPad Prism software. A statistical probability of $P<0.05$ was considered significant.

Results

Effect of Nano in delivering SOD1 to E-47 cells

We previously reported that Nano effectively delivers SOD1 to myocytes and endothelial cells (Natarajan et al., 2017; Saraswathi et al., 2016). Here, we tested whether Nano effectively delivers active SOD1 to cultured E-47 cells. Our data show that native SOD1 was not taken up by the cells, as the amount of intracellular SOD-1 did not rise above background levels. As noted in Fig. 1A, the top protein band in the Nano treated group represents endogenous human SOD1 expressed by E-47 cells. The protein band just below it is the bovine SOD-1 delivered by Nano. Thus, only Nano-treated cells exhibited a significant increase in SOD1 protein content, compared with control cells. To determine whether SOD1 delivered via Nano was also biologically active, we measured DCF fluorescence, a marker of oxidative stress. As shown in Fig 1B, treatment of E47 cells with either ethanol or linoleic acid (LA), showed only a numerical increase in oxidant stress, as assessed by DCF fluorescence. However, when we treated cells with both ethanol and LA, we observed a robust rise in DCF fluorescence, which was significantly blunted by a 6 h pretreatment with Nano, indicating that Nano is not only effective in delivering SOD1 to the cells but also in attenuating ethanol+LA-induced oxidative stress.

Effect of Nano on ethanol-induced hepatic steatosis

We next performed an ethanol feeding study in mice. H&E-stained liver sections from control mice and Cont+Nano-treated mice showed normal histology with an intact lobular architecture, free of steatosis (Fig. 2A&B). Mice subjected to 4 weeks of ethanol feeding alone developed changes in the centrilobular portions of their hepatic lobules characterized by reactive hepatocyte cytoplasmic and nuclear enlargement in a perivenular distribution ringed by cells with mild to moderate mixed macrovesicular and microvesicular steatosis, concentrated in a map-like pattern (Fig. 2C). Ethanol-fed animals treated with the nanoformulated SOD-1 showed a modest decrease in the aforementioned cytologic changes and the degree of steatosis (Fig. 2D). Quantification of liver triglycerides supported our histological findings, as liver triglycerides were greater than three-fold higher in ethanol-fed mice than in controls. Nano-treated ethanol-fed mice exhibited 22% lower hepatic triglycerides than untreated ethanol-fed mice (Fig. 2E). Interestingly, ALT, a plasma marker of liver injury, was unaltered in ethanol- and ethanol+Nano-treated mice (Fig. 2F). Further, liver SOD1 activity was unaltered among different groups (Fig. 2G). Liver SOD1 content was also not altered by Nano treatment. Moreover, the levels of hepatic TBARS, a measure of oxidative stress, were not altered in ethanol or ethanol+Nano-treated mice (not shown).

We noted that ethanol-fed mice exhibited 25% mortality. Out of eight mice in the ethanol-fed group, two died during ethanol feeding, whereas all mice in ethanol+Nano-treated group survived until sacrifice. To determine whether Nano alters ethanol metabolism, we attempted to measure ethanol and acetaldehyde in plasma samples by gas chromatography. We detected neither ethanol nor acetaldehyde in our samples. This is likely due, in part, to the fact that we fasted the mice for 5 h before sacrifice, which probably allowed complete ethanol clearance from the plasma. In fact, ethanol is considered to be undetectable in human blood 5–6 h after discontinuation of ethanol intake (Laposata, 1999). We next measured the hepatic contents of ADH1 and CYP2E1 (Fig. 3A–C). ADH1 protein level was not altered significantly in ET-fed mice compared to controls. However, there was a significant increase in ADH1 protein levels in ET+Nano-treated mice compared to control diet-fed mice ($P<0.01$) and ethanol-treated mice ($P<0.05$) (Fig 3A&B). Regarding CYP2E1, the protein level of this enzyme was significantly increased in both ET- and ET+Nano-treated mice compared to controls ($P<0.001$). No difference was noted between ET- and ET +Nano-treated mice (Fig. 3A&C). Together, these data suggest that the levels of ET-metabolizing enzymes are increased in both ET- and ET+Nano-treated mice with a slightly higher increase in ET+Nano-treated mice. However, further studies on enzyme activity and particularly in the fed condition are needed to determine the precise role of Nano in modulating ethanol metabolism.

Effect of Nano on ethanol-induced hepatic inflammation

To determine whether Nano treatment attenuated hepatic inflammation, we measured the levels of mRNAs encoding macrophage and inflammatory markers. As shown in Fig. 4A, the mRNA level of *Cd68*, a macrophage marker, was not significantly increased in ethanol-fed mice compared to controls. However, we noted that liver *Cd68 mRNA* was significantly lower in ethanol+Nano-treated mice compared with ethanol-fed mice. Interestingly, the mRNA levels of *Ccl2* and *Mmp12*, the inflammatory markers, were significantly elevated in

ethanol-fed mice compared with controls ($P<0.05$), but Nano treatment reduced their content (Fig. 4B&C). The mRNA encoding IL6 (a hepatoprotective cytokine) and TNFα did not change in livers of any of the four treatment groups (Fig. 4D&E). Immunofluorescence analysis for MCP1 expression revealed a prominent increase in ethanol-fed mice over controls which was attenuated by Nano treatment (Fig. 5A–D). MCP-1 staining was noted in all cell types as well as the extracellular matrix. Although it is unclear whether Kupffer cells or parenchymal cells are the major source of MCP-1, these data indicate that MCP-1 protein is increased overall in ethanol-fed mice and that Nano was effective in reducing hepatic MCP-1 level. Not only did the hepatic levels of MCP1 rise in ET-fed mice, but also its plasma levels increased in ethanol-fed mice and this rise was blunted in Nano-treated mice (Fig. 5E). Plasma TNFα levels were highly variable and there were no significant alterations in TNF-α among the four groups (Fig. 5F). We also analyzed whether the hepatic expression of CCR2, the receptor for MCP1, is differentially altered in ethanol and/or Nano-treated mice. We noted a considerable rise in CCR2 staining in ethanol-fed mice compared with controls, which was reduced in ET+Nano-treated mice (Fig. 6A–D).

Effect of Nano on markers of lipid metabolism

Because Nano treatment attenuated lipid accumulation in ethanol-fed mice (Fig 2D), we determined whether it affected hepatic markers of lipid metabolism. Previous studies demonstrated that ethanol feeding increases SREBP1c, a transcription factor that stimulates lipogenesis (Ji & Kaplowitz, 2003; You, Fischer, Deeg, & Crabb, 2002). Here, we noted that ethanol feeding caused a significant rise in SREBP1, compared with Cont+Nano-treated mice but not with untreated control diet fed mice. The latter rise was not observed in ethanol +Nano-treated mice. Ethanol feeding caused a trend towards an increase but not a significant rise in FASN whereas the level of this enzyme in ethanol+Nano-treated mice was equal to controls (Fig. 7A–C).

Effect of Nano on AMPK signaling

AMPK signaling regulates inflammation and metabolism. In fact, we previously reported that Nano promotes AMPK signaling in skeletal muscle (Natarajan et al., 2017). Therefore, we analyzed AMPK phosphorylation in liver. Interestingly, AMPK phosphorylation was significantly higher in ethanol+Nano-treated mice compared with both control and ethanol-fed mice. In addition, phosphorylation of ACC, a downstream target of phosphorylated AMPK, was significantly higher in livers of ethanol+Nano-treated mice than controls (Fig. 8A–E). These data suggest that AMPK has a role in mediating the anti-steatotic and/or anti-inflammatory effects of Nano.

Effects of Nano on AT inflammation

Evidence suggests that AT inflammation contributes to AALD (Fulham & Mandrekar, 2016). Chronic ethanol feeding promotes AT inflammation in female mice (Sebastian et al., 2011) and rats (X. Chen et al., 2009; Kang et al., 2007; Lin, Yang, Zeldin, & Diehl, 1998). Here, we quantified visceral AT samples for macrophage and inflammatory markers and noted that the mRNA level of *F4/80*, a macrophage marker, was not significantly altered in AT from the four animal groups (Fig. 9A). Although the expression of *Clec10a*, a marker of pro-inflammatory macrophages (Gaur, Myles, Misra, & Aggarwal, 2017; Heger et al., 2018)

did not rise significantly in ethanol-fed mice compared to control mice, its expression was significantly higher in ethanol-fed mice compared to Cont+Nano-treated mice. (Fig. 9B). On the other hand, ET+Nano-treated mice showed a reduction in *Clec10a* levels. Interestingly, ethanol+Nano-treated mice showed a significant rise in *Arg1* mRNA compared with control mice (Fig. 9C). *Arg1* is a marker of anti-inflammatory M2 macrophages (Zeyda et al., 2010; H. Zhao et al., 2018). We did not see an increase in inflammatory markers in particular, C*cl2*, upon ethanol feeding. However, Nano treatment led to a trend towards a decrease in *Ccl2* compared to ethanol-fed mice (Fig. 9D). Of note, AT from ethanol+Nano-treated mice showed a significant rise in *IL-6* mRNA compared with control mice (Fig. 9E). IL-6 is considered to be hepatoprotective against ethanol-induced injury (Hong et al., 2002; Zhang et al., 2010). We measured visceral AT mass to determine whether changes in AT mass may account for the changes in AT inflammatory markers and/or hepatic steatosis. As expected, ethanol feeding reduced AT mass compared to control (2.8 ± 0.5 and 2.2 ± 0.2 g/body weight in control and ethanol-fed mice, respectively) and Nano treatment in ethanol-fed mice led to a greater decrease (1.6 ± 0.2 g/body weight). However, the difference in AT mass among different groups did not reach significance (not shown). Taken together, ethanol feeding by itself did not result in a significant increase in the expression of inflammatory markers in AT compared to control mice. However, Nano treatment led to an overall reduction in AT inflammation as evidenced by increased expression of *Arg1*, a marker of M2 anti-inflammatory macrophages and that of *Il6*, a protective cytokine against ethanol-induced injury.

Discussion

Here, we used a novel nanoformulated SOD1, to determine whether ethanol-induced steatosis and/or inflammation can be ablated or eliminated in liver and AT of chronically ethanol-fed mice. Nano was effectively taken up by E47 cells and its uptake attenuated ethanol+LA-induced oxidative stress in these CYP2E1-expressing cells. Our *in vivo* experiments with ethanol-fed mice revealed that hepatic steatosis and inflammation were attenuated by Nano treatment. Moreover, there was a rather robust rise in hepatic pAMPK in ethanol+Nano-treated mice compared with untreated ethanol-fed mice. In the AT, chronic ethanol feeding caused no change in inflammatory markers compared to controls. However, Nano treatment favorably altered AT inflammatory markers compared to ethanol-fed mice. Together, our data suggest that Nano effectively attenuates ethanol-induced liver injury. This latter effect may be mediated partly via increased AMPK signaling.

We previously reported that Nano treatment to mice effectively diminishes NAFLD induced by a high fat diet (Perriotte-Olson et al., 2016). In order to delineate the effect of Nano on AALD, we performed the current ethanol feeding experiment under the same conditions. For example, we used male mice and euthanized them after 5 h of fasting and showed that Nano partly reduces ethanol-induced fatty liver disease. Ethanol-induced increases in inflammatory markers were greatly reduced upon Nano treatment. Steatosis leads to tissue injury when associated with inflammation. For example, steatosis in the absence of inflammation in some cases, promotes or does not affect liver regeneration after partial hepatectomy (Picard et al., 2002; Rao, Papreddy, Abecassis, & Hashimoto, 2001; Sydor et

al., 2013). Thus, although Nano did not completely ablate steatosis, it reduced hepatic inflammation suggesting that Nano can be an effective treatment in ameliorating AALD.

Although Nano administration is expected to increase SOD1 content in liver, we detected no increase in SOD1 protein or its activity in liver upon Nano treatment. One plausible reason is that mice were euthanized a day after injecting the last dose of Nano. Therefore, a time course study is needed to better determine the effect of Nano in increasing SOD1 protein and/or activity in liver. However, our *in vitro* studies in E47 HepG2 cells clearly show that Nano is effective in delivering SOD1 to hepatocytes and also in reducing oxidative stress.

Several lines of evidence suggest that ethanol-induced hepatic inflammation is characterized by an increase in MCP-1 in liver (Mandrekar, Ambade, Lim, Szabo, & Catalano, 2011; Na et al., 2015; Nath et al., 2011). Our data confirmed these findings and showed an increase in mRNA encoding MCP-1 (*Ccl2*) and its protein levels in ethanol-fed mice. Interestingly, Nano treatment caused a remarkable decrease in *Ccl2* expression. As reported earlier (Horiguchi et al., 2008), we noted an increase in the level of CCR2, an MCP-1 receptor and a marker of monocyte/macrophages in ethanolfed mice. Such an increase was less evident in ET+Nano-treated mice, indicating a reduction in hepatic inflammation. In addition to MCP-1, MMPs play an important role in the development of AALD. For example, Koken *et al.* have shown that long-term ethanol feeding increases pro-MMP9 levels which were brought back to normal levels by vitamin E treatment (Koken, Gursoy, & Kahraman, 2010). Here, we provide novel evidence that not only MCP-1, but also the mRNA level of *Mmp12* was increased upon ethanol feeding. Moreover, our data show that Nano treatment was effective in reducing *Mmp12* expression in liver. We should also point out that, in addition to hepatic inflammatory markers, plasma MCP-1 level was attenuated by Nano treatment. (Fig 5E). Taken together, analysis of inflammatory markers in liver and plasma clearly suggests that Nano treatment effectively attenuates hepatic and systemic inflammation caused by chronic ethanol administration.

Regarding potential mechanisms, we noted that Nano promotes AMPK signaling in liver. We previously reported that Nano enhances AMPK signaling in skeletal muscle of lean and obese mice (Natarajan et al., 2017). Ethanol by itself has been shown to increase or reduce AMPK signaling, depending on the experimental conditions (Everitt et al., 2013; Qin & Tian, 2010; Shearn et al., 2013; Shen, Liang, Rogers, Rideout, & You, 2010). Here we report that ethanol did not alter AMPK phosphorylation significantly but ethanol+Nano-treated mice showed a remarkable increase in the phosphorylation of AMPK as well as its downstream target, ACC, suggesting that AMPK signaling plays a role in mediating Nano effects on liver lipid metabolism and/or inflammation. In fact, AMPK modulates lipid metabolism by inhibiting lipogenesis. For example, phosphorylation of ACC inhibits its activity, which leads to a reduction in fatty acid synthesis. Moreover, AMPK activation has been shown to inhibit SREBP1 expression (Li, Li, Wang, & Yang, 2014; Nammi & Roufogalis, 2013), which, in turn, can reduce hepatic steatosis. In fact, our data show that increased AMPK phosphorylation is associated with a reduction in SREBP1 protein levels in ethanol+Nano treated mice compared with ethanol-fed mice. AMPK also inhibits inflammatory processes by blocking NF-κB (Salminen, Hyttinen, & Kaarniranta, 2011).

Together, our data suggest that improvements in hepatic steatosis and inflammation seen in ethanol+Nano-treated mice could be mediated via increased AMPK signaling.

Ethanol increases AT inflammation, as reported in a number of studies (X. Chen et al., 2009; Kang et al., 2007; Lin et al., 1998; Sebastian et al., 2011). However, our data show that markers of AT inflammation were not altered significantly after 4 wk of chronic ethanol feeding. This may be attributed to the experimental conditions. For example, previous studies showing ethanol-induced AT inflammation were conducted in rats (X. Chen et al., 2009; Kang et al., 2007; Lin et al., 1998) or female mice (Sebastian et al., 2011). In fact, a recent report by Fulham *et al* suggests that the effect of ethanol on AT inflammation is gender-dependent (Fulham & Mandrekar, 2016). Regardless of the extent of AT inflammation by ethanol feeding, our data show that ethanol+Nano-treated mice expressed higher levels of *Il6* and *Arg1* mRNAs in AT. IL6 is a pleiotropic cytokine that reportedly exerts beneficial effects against ethanol-induced liver injury (Hong et al., 2002; Zhang et al., 2010). Moreover, *Arg1*, which encodes arginase is a marker of M2 anti-inflammatory macrophages (Zeyda et al., 2010; H. Zhao et al., 2018) and our data show a significant upregulation of *Arg1* in AT in ethanol+Nano-treated mice compared with control. Overall, our data suggest that Nano exerts favorable effects in AT.

Our data suggest that nanoformulated SOD1 is effective in ameliorating AALD and this effect may be mediated partly via hepatic AMPK signaling. We hasten to point out that here, ethanol feeding led to only mild to moderate tissue injury as we failed to detect elevated plasma ALT, a marker of liver injury. Moreover, AT inflammatory markers were not significantly altered in ethanol-alone fed mice. It is well-known that ethanol induces liver injury to a greater extent in female mice than male mice, which were used here. Moreover, ethanol-induced changes in AT appears to be gender specific as well (Fulham & Mandrekar, 2016). Therefore, to better evaluate the effectiveness of Nano in AALD and/or AT inflammation, studies in female mice fed an ethanol diet for a longer period or in mice exposed to chronic+acute ethanol feeding (NIAAA model), is needed.

Acknowledgments

This project was supported by the NIH-National Institute on Alcoholism (1R21 AA025445) and partly by the Bly Memorial Research Fund and the Nebraska Research Initiatives Seed Grant (V.S). A.V.K. was partly supported by Carolina Partnership, a strategic partnership between the University of North Carolina at Chapel Hill Eshelman School of Pharmacy and the University Cancer Research Fund through the Lineberger Comprehensive Cancer Center. We thank Dr. Dahn Clemens for providing us the E47 cells for our study. This study is the result of work conducted with the resources and the facilities at the VA Nebraska-Western Iowa Health Care System, Omaha, Nebraska.

Funding. This project was supported by the NIH-National Institute on Alcoholism (1R21 AA025445) and partly by the Bly Memorial Research Fund and Nebraska Research Initiatives Seed Grant (V.S). A.V.K. was partly supported by Carolina Partnership, a strategic partnership between the University of North Carolina at Chapel Hill Eshelman School of Pharmacy and the University Cancer Research Fund through the Lineberger Comprehensive Cancer Center.

References

Abdelmegeed MA, Banerjee A, Jang S, Yoo SH, Yun JW, Gonzalez FJ, …Song BJ (2013). CYP2E1 potentiates binge alcohol-induced gut leakiness, steatohepatitis, and apoptosis. Free Radic Biol Med, 65, 1238–1245. doi:10.1016/j.freeradbiomed.2013.09.009 [PubMed: 24064383]

Boveris A, Fraga CG, Varsavsky AI, & Koch OR (1983). Increased chemiluminescence and superoxide production in the liver of chronically ethanol-treated rats. Arch Biochem Biophys, 227(2), 534–541. [PubMed: 6320728]

Chen LH, Xi S, & Cohen DA (1995). Liver antioxidant defenses in mice fed ethanol and the AIN-76A diet. Alcohol, 12(5), 453–457. [PubMed: 8519441]

Chen X, Sebastian BM, Tang H, McMullen MM, Axhemi A, Jacobsen DW, & Nagy LE (2009). Taurine supplementation prevents ethanol-induced decrease in serum adiponectin and reduces hepatic steatosis in rats. Hepatology, 49(5), 1554–1562. doi:10.1002/hep.22811 [PubMed: 19296466]

Ekstrom G, & Ingelman-Sundberg M (1989). Rat liver microsomal NADPH-supported oxidase activity and lipid peroxidation dependent on ethanol-inducible cytochrome P-450 (P-450IIE1). Biochem Pharmacol, 38(8), 1313–1319. [PubMed: 2495801]

Eto Y, Yoshioka Y, Mukai Y, Okada N, & Nakagawa S (2008). Development of PEGylated adenovirus vector with targeting ligand. Int J Pharm, 354(1–2), 3–8. doi:10.1016/j.ijpharm.2007.08.025 [PubMed: 17904316]

Everitt H, Hu M, Ajmo JM, Rogers CQ, Liang X, Zhang R, … You M (2013). Ethanol administration exacerbates the abnormalities in hepatic lipid oxidation in genetically obese mice. Am J Physiol Gastrointest Liver Physiol, 304(1), G38–47. doi:10.1152/ajpgi.00309.2012 [PubMed: 23139221]

Folch J, Lees M, & Sloane Stanley GH (1957). A simple method for the isolation and purification of total lipides from animal tissues. J Biol Chem, 226(1), 497–509. [PubMed: 13428781]

Fulham MA, & Mandrekar P (2016). Sexual Dimorphism in Alcohol Induced Adipose Inflammation Relates to Liver Injury. PLoS One, 11(10), e0164225. doi:10.1371/journal.pone.0164225 [PubMed: 27711160]

Gaur P, Myles A, Misra R, & Aggarwal A (2017). Intermediate monocytes are increased in enthesitis-related arthritis, a category of juvenile idiopathic arthritis. Clin Exp Immunol, 187(2), 234–241. doi:10.1111/cei.12880 [PubMed: 27706807]

Gotoh N, & Niki E (1992). Rates of interactions of superoxide with vitamin E, vitamin C and related compounds as measured by chemiluminescence. Biochim Biophys Acta, 1115(3), 201–207. [PubMed: 1310874]

Heger L, Balk S, Luhr JJ, Heidkamp GF, Lehmann CHK, Hatscher L, … Dudziak D (2018). CLEC10A Is a Specific Marker for Human CD1c(+) Dendritic Cells and Enhances Their Toll-Like Receptor 7/8-Induced Cytokine Secretion. Front Immunol, 9, 744. doi:10.3389/fimmu.2018.00744 [PubMed: 29755453]

Hong F, Kim WH, Tian Z, Jaruga B, Ishac E, Shen X, & Gao B (2002). Elevated interleukin-6 during ethanol consumption acts as a potential endogenous protective cytokine against ethanol-induced apoptosis in the liver: involvement of induction of Bcl-2 and Bcl-x(L) proteins. Oncogene, 21(1), 32–43. doi:10.1038/sj.onc.1205016 [PubMed: 11791174]

Horiguchi N, Wang L, Mukhopadhyay P, Park O, Jeong WI, Lafdil F, … Gao B (2008). Cell type-dependent pro- and anti-inflammatory role of signal transducer and activator of transcription 3 in alcoholic liver injury. Gastroenterology, 134(4), 1148–1158. doi:10.1053/j.gastro.2008.01.016 [PubMed: 18395093]

Ji C, & Kaplowitz N (2003). Betaine decreases hyperhomocysteinemia, endoplasmic reticulum stress, and liver injury in alcohol-fed mice. Gastroenterology, 124(5), 1488–1499. [PubMed: 12730887]

Kang L, Sebastian BM, Pritchard MT, Pratt BT, Previs SF, & Nagy LE (2007). Chronic ethanol-induced insulin resistance is associated with macrophage infiltration into adipose tissue and altered expression of adipocytokines. Alcohol Clin Exp Res, 31(9), 1581–1588. doi:10.1111/j.1530-0277.2007.00452.x [PubMed: 17624994]

Kessova IG, & Cederbaum AI (2007). Mitochondrial alterations in livers of Sod1−/− mice fed alcohol. Free Radic Biol Med, 42(10), 1470–1480. doi:10.1016/j.freeradbiomed.2007.01.044 [PubMed: 17448893]

Kessova IG, Ho YS, Thung S, & Cederbaum AI (2003). Alcohol-induced liver injury in mice lacking Cu, Zn-superoxide dismutase. Hepatology, 38(5), 1136–1145. doi:10.1053/jhep.2003.50450 [PubMed: 14578852]

Kirpich IA, Feng W, Wang Y, Liu Y, Barker DF, Barve SS, & McClain CJ (2012). The type of dietary fat modulates intestinal tight junction integrity, gut permeability, and hepatic toll-like receptor expression in a mouse model of alcoholic liver disease. Alcohol Clin Exp Res, 36(5), 835–846. doi:10.1111/j.1530-0277.2011.01673.x [PubMed: 22150547]

Koch OR, Galeotti T, Bartoli GM, & Boveris A (1991). Alcohol-induced oxidative stress in rat liver. Xenobiotica, 21(8), 1077–1084. [PubMed: 1776278]

Koken T, Gursoy F, & Kahraman A (2010). Long-term alcohol consumption increases pro-matrix metalloproteinase-9 levels via oxidative stress. J Med Toxicol, 6(2), 126–130. doi:10.1007/s13181-010-0081-y [PubMed: 20405265]

Laethem RM, Balazy M, Falck JR, Laethem CL, & Koop DR (1993). Formation of 19(S)-, 19(R)-, and 18(R)-hydroxyeicosatetraenoic acids by alcohol-inducible cytochrome P450 2E1. J Biol Chem, 268(17), 12912–12918. [PubMed: 8509425]

Laposata M (1999). Assessment of ethanol intake. Current tests and new assays on the horizon. Am J Clin Pathol, 112(4), 443–450. [PubMed: 10510667]

Li W, Li Y, Wang Q, & Yang Y (2014). Crude extracts from Lycium barbarum suppress SREBP-1c expression and prevent diet-induced fatty liver through AMPK activation. Biomed Res Int, 2014, 196198. doi:10.1155/2014/196198 [PubMed: 25013763]

Lieber CS, & DeCarli LM (1989). Liquid diet technique of ethanol administration: 1989 update. Alcohol Alcohol, 24(3), 197–211. [PubMed: 2667528]

Lin HZ, Yang SQ, Zeldin G, & Diehl AM (1998). Chronic ethanol consumption induces the production of tumor necrosis factor-alpha and related cytokines in liver and adipose tissue. Alcohol Clin Exp Res, 22(5 Suppl), 231S–237S. [PubMed: 9727642]

Mandrekar P, Ambade A, Lim A, Szabo G, & Catalano D (2011). An essential role for monocyte chemoattractant protein-1 in alcoholic liver injury: regulation of proinflammatory cytokines and hepatic steatosis in mice. Hepatology, 54(6), 2185–2197. doi:10.1002/hep.24599 [PubMed: 21826694]

Manickam DS, Brynskikh AM, Kopanic JL, Sorgen PL, Klyachko NL, Batrakova EV, … Kabanov AV (2012). Well-defined cross-linked antioxidant nanozymes for treatment of ischemic brain injury. J Control Release, 162(3), 636–645. doi:S0168–3659(12)00615–3 [pii] 10.1016/j.jconrel.2012.07.044 [PubMed: 22902590]

Mezey E, Potter JJ, Rennie-Tankersley L, Caballeria J, & Pares A (2004). A randomized placebo controlled trial of vitamin E for alcoholic hepatitis. J Hepatol, 40(1), 40–46. [PubMed: 14672612]

Mihara M, & Uchiyama M (1978). Determination of malonaldehyde precursor in tissues by thiobarbituric acid test. Anal Biochem, 86(1), 271–278. [PubMed: 655387]

Na TY, Han YH, Ka NL, Park HS, Kang YP, Kwon SW, … Lee MO (2015). 22-S-Hydroxycholesterol protects against ethanol-induced liver injury by blocking the auto/paracrine activation of MCP-1 mediated by LXRalpha. J Pathol, 235(5), 710–720. doi:10.1002/path.4494 [PubMed: 25557254]

Nammi S, & Roufogalis BD (2013). Light-to-moderate ethanol feeding augments AMPK-alpha phosphorylation and attenuates SREBP-1 expression in the liver of rats. J Pharm Pharm Sci, 16(2), 342–351. [PubMed: 23958203]

Natarajan G, Perriotte-Olson C, Bhinderwala F, Powers R, Desouza CV, Talmon GA, … Saraswathi V (2017). Nanoformulated copper/zinc superoxide dismutase exerts differential effects on glucose vs lipid homeostasis depending on the diet composition possibly via altered AMPK signaling. Transl Res, 188, 10–26. doi:10.1016/j.trsl.2017.08.002 [PubMed: 28867395]

Nath B, Levin I, Csak T, Petrasek J, Mueller C, Kodys K, … Szabo G (2011). Hepatocyte-specific hypoxia-inducible factor-1alpha is a determinant of lipid accumulation and liver injury in alcohol-induced steatosis in mice. Hepatology, 53(5), 1526–1537. doi:10.1002/hep.24256 [PubMed: 21520168]

Ouchi A, Ishikura M, Konishi K, Nagaoka S, & Mukai K (2009). Kinetic study of the prooxidant effect of alpha-tocopherol. Hydrogen abstraction from lipids by alpha-tocopheroxyl radical. Lipids, 44(10), 935–943. doi:10.1007/s11745-009-3339-x [PubMed: 19763654]

Perriotte-Olson C, Adi N, Manickam DS, Westwood RA, Desouza CV, Natarajan G, … Saraswathi V (2016). Nanoformulated copper/zinc superoxide dismutase reduces adipose inflammation in obesity. Obesity (Silver Spring), 24(1), 148–156. doi:10.1002/oby.21348 [PubMed: 26612356]

Picard C, Lambotte L, Starkel P, Sempoux C, Saliez A, Van den Berge V, & Horsmans Y (2002). Steatosis is not sufficient to cause an impaired regenerative response after partial hepatectomy in rats. J Hepatol, 36(5), 645–652. [PubMed: 11983448]

Polavarapu R, Spitz DR, Sim JE, Follansbee MH, Oberley LW, Rahemtulla A, & Nanji AA (1998). Increased lipid peroxidation and impaired antioxidant enzyme function is associated with pathological liver injury in experimental alcoholic liver disease in rats fed diets high in corn oil and fish oil. Hepatology, 27(5), 1317–1323. doi:10.1002/hep.510270518 [PubMed: 9581686]

Qin Y, & Tian YP (2010). Exploring the molecular mechanisms underlying the potentiation of exogenous growth hormone on alcohol-induced fatty liver diseases in mice. J Transl Med, 8, 120. doi:10.1186/1479-5876-8-120 [PubMed: 21087523]

Rao MS, Papreddy K, Abecassis M, & Hashimoto T (2001). Regeneration of liver with marked fatty change following partial hepatectomy in rats. Dig Dis Sci, 46(9), 1821–1826. [PubMed: 11575431]

Rosenbaugh EG, Roat JW, Gao L, Yang RF, Manickam DS, Yin JX, … Zimmerman MC (2010). The attenuation of central angiotensin II-dependent pressor response and intra-neuronal signaling by intracarotid injection of nanoformulated copper/zinc superoxide dismutase. Biomaterials, 31(19), 5218–5226. doi:10.1016/j.biomaterials.2010.03.026 [PubMed: 20378166]

Salminen A, Hyttinen JM, & Kaarniranta K (2011). AMP-activated protein kinase inhibits NF-kappaB signaling and inflammation: impact on healthspan and lifespan. J Mol Med (Berl), 89(7), 667–676. doi:10.1007/s00109-011-0748-0 [PubMed: 21431325]

Saraswathi V, Ganesan M, Perriotte-Olson C, Manickam DS, Westwood RA, Zimmerman MC, … Kabanov AV (2016). Nanoformulated copper/zinc superoxide dismutase attenuates vascular cell activation and aortic inflammation in obesity. Biochem Biophys Res Commun, 469(3), 495–500. doi:10.1016/j.bbrc.2015.12.027 [PubMed: 26692492]

Saraswathi V, & Hasty AH (2009). Inhibition of long-chain acyl coenzyme A synthetases during fatty acid loading induces lipotoxicity in macrophages. Arterioscler Thromb Vasc Biol, 29(11), 1937–1943. doi:ATVBAHA.109.195362 [pii] 10.1161/ATVBAHA.109.195362 [PubMed: 19679826]

Saraswathi V, Wu G, Toborek M, & Hennig B (2004). Linoleic acid-induced endothelial activation: role of calcium and peroxynitrite signaling. J Lipid Res, 45(5), 794–804. doi:10.1194/jlr.M300497-JLR200 M300497-JLR200 [pii] [PubMed: 14993245]

Sebastian BM, Roychowdhury S, Tang H, Hillian AD, Feldstein AE, Stahl GL, … Nagy LE (2011). Identification of a cytochrome P4502E1/Bid/C1q-dependent axis mediating inflammation in adipose tissue after chronic ethanol feeding to mice. J Biol Chem, 286(41), 35989–35997. doi:10.1074/jbc.M111.254201 [PubMed: 21856753]

Shearn CT, Smathers RL, Jiang H, Orlicky DJ, Maclean KN, & Petersen DR (2013). Increased dietary fat contributes to dysregulation of the LKB1/AMPK pathway and increased damage in a mouse model of early-stage ethanol-mediated steatosis. J Nutr Biochem, 24(8), 1436–1445. doi:10.1016/j.jnutbio.2012.12.002 [PubMed: 23465594]

Shen Z, Liang X, Rogers CQ, Rideout D, & You M (2010). Involvement of adiponectin-SIRT1-AMPK signaling in the protective action of rosiglitazone against alcoholic fatty liver in mice. Am J Physiol Gastrointest Liver Physiol, 298(3), G364–374. doi:10.1152/ajpgi.00456.2009 [PubMed: 20007851]

Stewart S, Prince M, Bassendine M, Hudson M, James O, Jones D, … Day CP (2007). A randomized trial of antioxidant therapy alone or with corticosteroids in acute alcoholic hepatitis. J Hepatol, 47(2), 277–283. doi:10.1016/j.jhep.2007.03.027 [PubMed: 17532088]

Stocker R (1999). The ambivalence of vitamin E in atherogenesis. Trends Biochem Sci, 24(6), 219–223. [PubMed: 10366846]

Sung M, Kim I, Park M, Whang Y, & Lee M (2004). Differential effects of dietary fatty acids on the regulation of CYP2E1 and protein kinase C in human hepatoma HepG2 cells. J Med Food, 7(2), 197–203. doi:10.1089/1096620041224157 [PubMed: 15298768]

Sydor S, Gu Y, Schlattjan M, Bechmann LP, Rauen U, Best J, … Canbay A (2013). Steatosis does not impair liver regeneration after partial hepatectomy. Lab Invest, 93(1), 20–30. doi:10.1038/labinvest.2012.142 [PubMed: 23069937]

Viswanathan S, Hammock BD, Newman JW, Meerarani P, Toborek M, & Hennig B (2003). Involvement of CYP 2C9 in mediating the proinflammatory effects of linoleic acid in vascular endothelial cells. J Am Coll Nutr, 22(6), 502–510. [PubMed: 14684755]

Wang X, Wu D, Yang L, Gan L, & Cederbaum AI (2013). Cytochrome P450 2E1 potentiates ethanol induction of hypoxia and HIF-1alpha in vivo. Free Radic Biol Med, 63, 175–186. doi:10.1016/j.freeradbiomed.2013.05.009 [PubMed: 23669278]

Wheeler MD, Kono H, Yin M, Rusyn I, Froh M, Connor HD, … Thurman RG (2001). Delivery of the Cu/Zn-superoxide dismutase gene with adenovirus reduces early alcohol-induced liver injury in rats. Gastroenterology, 120(5), 1241–1250. doi:10.1053/gast.2001.23253 [PubMed: 11266387]

White CW, Jackson JH, Abuchowski A, Kazo GM, Mimmack RF, Berger EM, … Repine JE (1989). Polyethylene glycol-attached antioxidant enzymes decrease pulmonary oxygen toxicity in rats. J Appl Physiol (1985), 66(2), 584–590. [PubMed: 2540139]

You M, Fischer M, Deeg MA, & Crabb DW (2002). Ethanol induces fatty acid synthesis pathways by activation of sterol regulatory element-binding protein (SREBP). J Biol Chem, 277(32), 29342–29347. doi:10.1074/jbc.M202411200 [PubMed: 12036955]

Zeyda M, Gollinger K, Kriehuber E, Kiefer FW, Neuhofer A, & Stulnig TM (2010). Newly identified adipose tissue macrophage populations in obesity with distinct chemokine and chemokine receptor expression. Int J Obes (Lond), 34(12), 1684–1694. doi:10.1038/ijo.2010.103 [PubMed: 20514049]

Zhang X, Tachibana S, Wang H, Hisada M, Williams GM, Gao B, & Sun Z (2010). Interleukin-6 is an important mediator for mitochondrial DNA repair after alcoholic liver injury in mice. Hepatology, 52(6), 2137–2147. doi:10.1002/hep.23909 [PubMed: 20931558]

Zhao H, Shang Q, Pan Z, Bai Y, Li Z, Zhang H, … Wang Q (2018). Exosomes From Adipose-Derived Stem Cells Attenuate Adipose Inflammation and Obesity Through Polarizing M2 Macrophages and Beiging in White Adipose Tissue. Diabetes, 67(2), 235–247. doi:10.2337/db17-0356 [PubMed: 29133512]

Zhao M, Matter K, Laissue JA, & Zimmermann A (1996). Copper/zinc and manganese superoxide dismutases in alcoholic liver disease: immunohistochemical quantitation. Histol Histopathol, 11(4), 899–907. [PubMed: 8930633]

Highlights

- Alcohol consumption is associated with liver injury and adipose tissue inflammation.
- Superoxide-mediated oxidative stress plays an important role in the development of alcohol-associated organ injury.
- Although a strong link exists between oxidative stress and alcohol-related liver injury, clinical trials using antioxidant vitamins and nutritional supplements were not effective in treating alcoholic liver disease.
- Nanoformulated antioxidant enzymes are emerging as effective tools in delivering active enzymes to injured cells and tissues.
- In the current study, we show that nanoformulated copper/zinc SOD (NanoSOD) is effective in attenuating chronic ethanol-induced liver injury and in favorably altering adipose tissue gene expression.

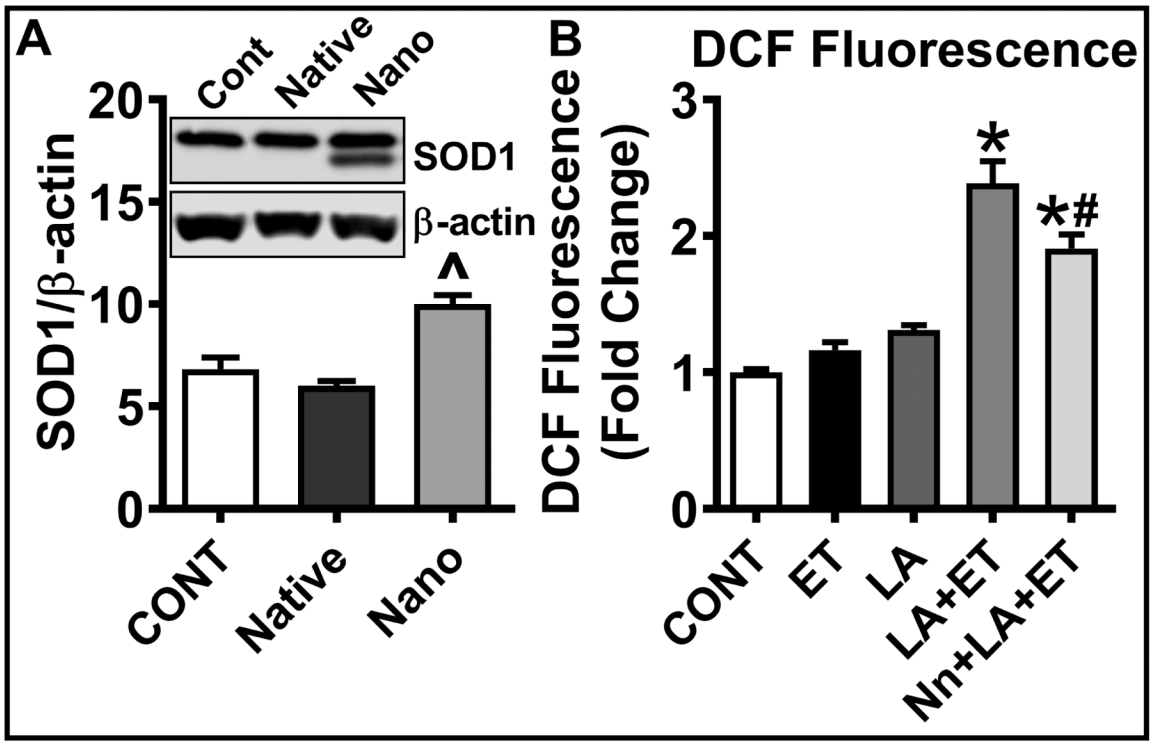

Fig. 1. Effect of Nano on SOD1 uptake and oxidative stress *in vitro*.

E47 hepatoma cells were treated with native- or nanoSOD for 6 h. After rinsing in PBS, cells were incubated with fresh medium overnight. Cell lysates were collected the following day for western blot analysis of SOD1 (A). E47 cells were pretreated with Nano for 6 h. After overnight incubation with fresh medium, cells were treated with ethanol (50 mM) and/or LA (120 μM) for 1 h. Cells were incubated with DCF for 30 min and DCF fluorescence were measured (B). Values are expressed as mean ± SEM of 3 independent experiments. ^P<0.001 vs all; *P<0.001 vs CONT, ET, LA; $^{\#}P$<0.01 vs LA+ET. CONT, control; ET, ethanol; LA, linoleic acid; Nn, NanoSOD.

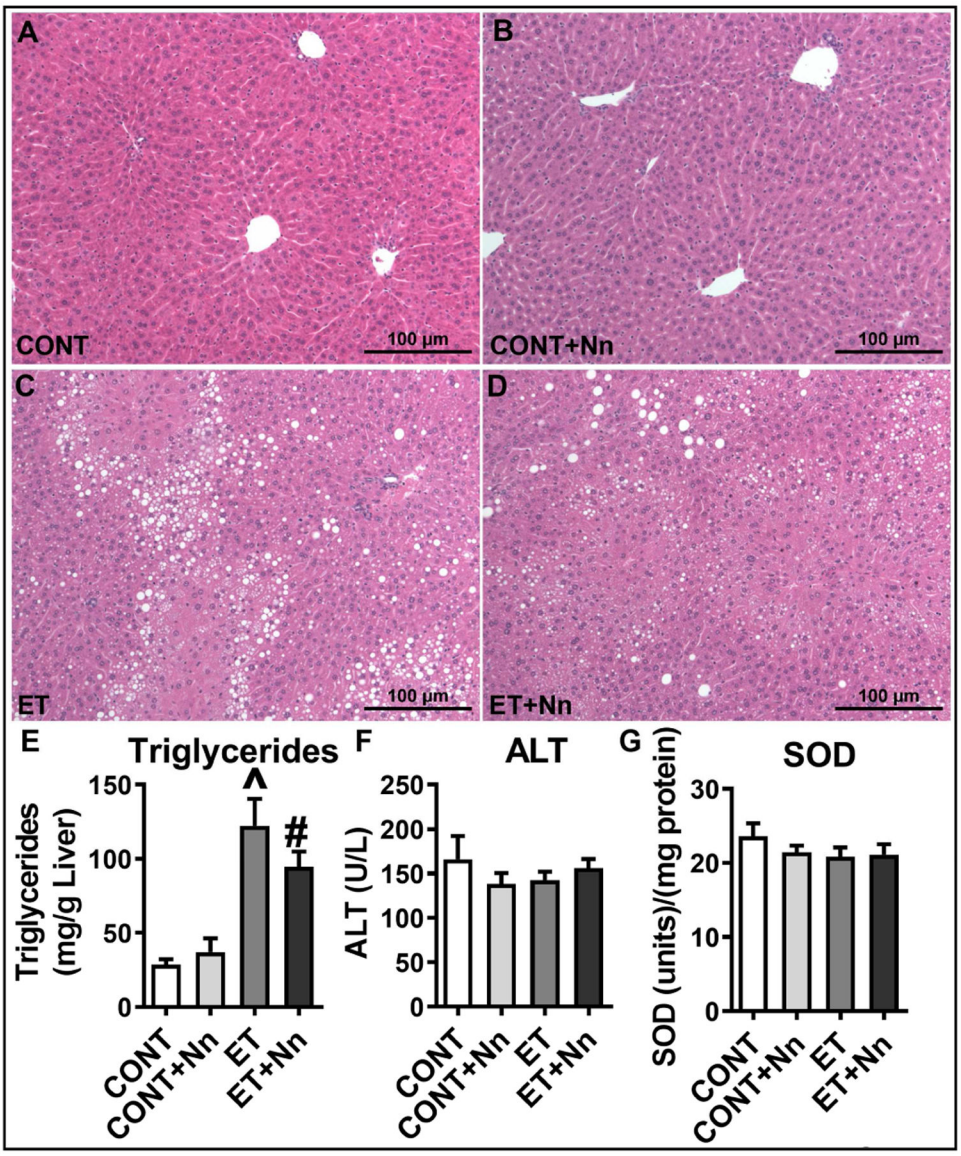

Fig. 2. Effect of Nano on ethanol-induced hepatic steatosis.

Liver sections (4 µm) were stained with hematoxylin and eosin. Pictures taken at 10X magnification using Nikon Eclipse 80i microscope (A-D). Hepatic triglyceride levels were quantified (E). Plasma ALT (F) and liver SOD1 activity were analyzed (G). Values are expressed as mean ± SEM of 6–8 samples in each group. $^{\#}P<0.01$, $^{\wedge}P<0.001$ vs CONT and CONT+Nn. CONT, control; ET, ethanol; Nn, NanoSOD.

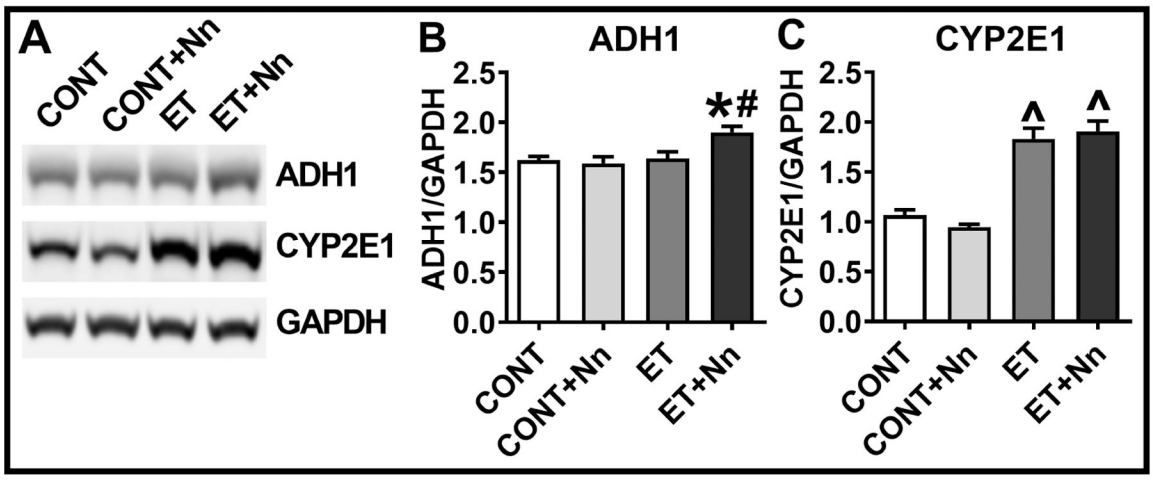

Fig. 3. Effect of Nano on the protein levels of alcohol metabolizing enzymes in liver.

Liver homogenates were subjected to western blot analysis for alcohol metabolizing enzymes, ADH1 and CYP2E1. Representative bands from each group are shown (A). Bands were quantified and values normalized to GAPDH. Protein levels of ADH1 (B) and CYP2E1 (C) are shown. Values are expressed as mean ± SEM of 6–8 samples in each group. $^{\#}P<0.01$ and $\wedge P<0.001$ vs CONT; $*P<0.05$ vs ET. CONT, control; ET, ethanol; Nn, Nano.

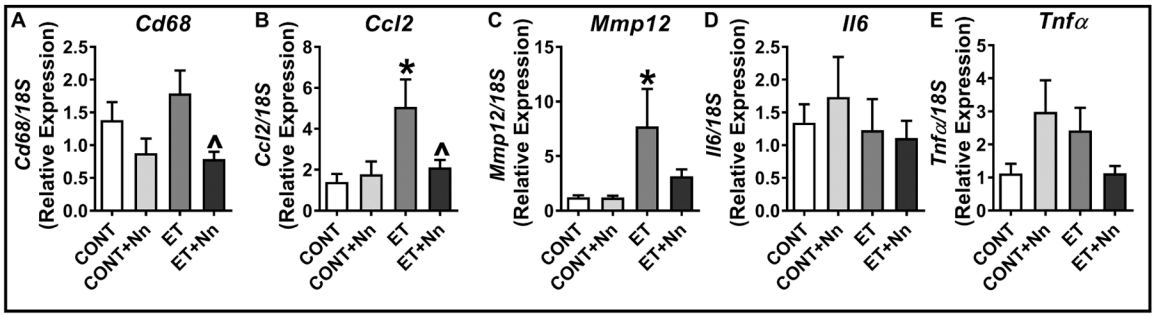

Fig. 4. Effect of Nano on the mRNA expression of inflammatory genes in liver.

Realtime PCR analysis was carried out in liver samples for the mRNA levels of macrophage and inflammatory markers (A-E). Values are normalized to 18S and expressed as mean ± SEM of 6–8 samples in each group. *P<0.05 vs CONT and CONT+Nn; ^P<0.05 vs ethanol. CONT, control; ET, ethanol; Nn, NanoSOD.

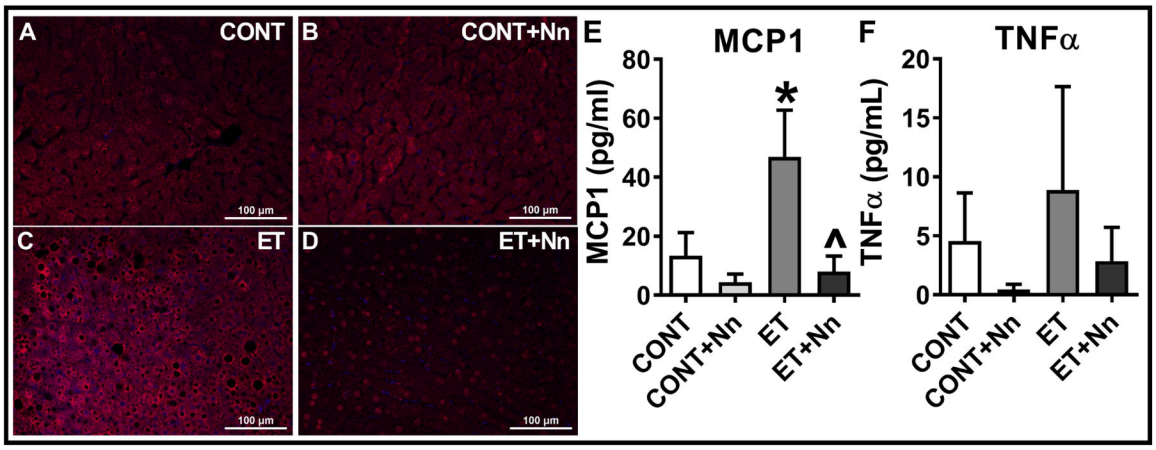

Fig. 5. Effect of Nano on the protein levels of inflammatory markers in liver and plasma.

Liver sections (4μm) were stained for MCP1 protein by immunofluorescence method. Representative pictures taken at 20X magnification are shown (A-D). Plasma levels of MCP1 and TNFα were determined by Luminex multiplex assay system (E&F). Values are expressed as mean ± SEM of 6–8 samples in each group. *P<0.05 vs CONT and P<0.01 vs CONT+Nn; ^P<0.05 vs ET. CONT, control; ET, ethanol; Nn, NanoSOD.

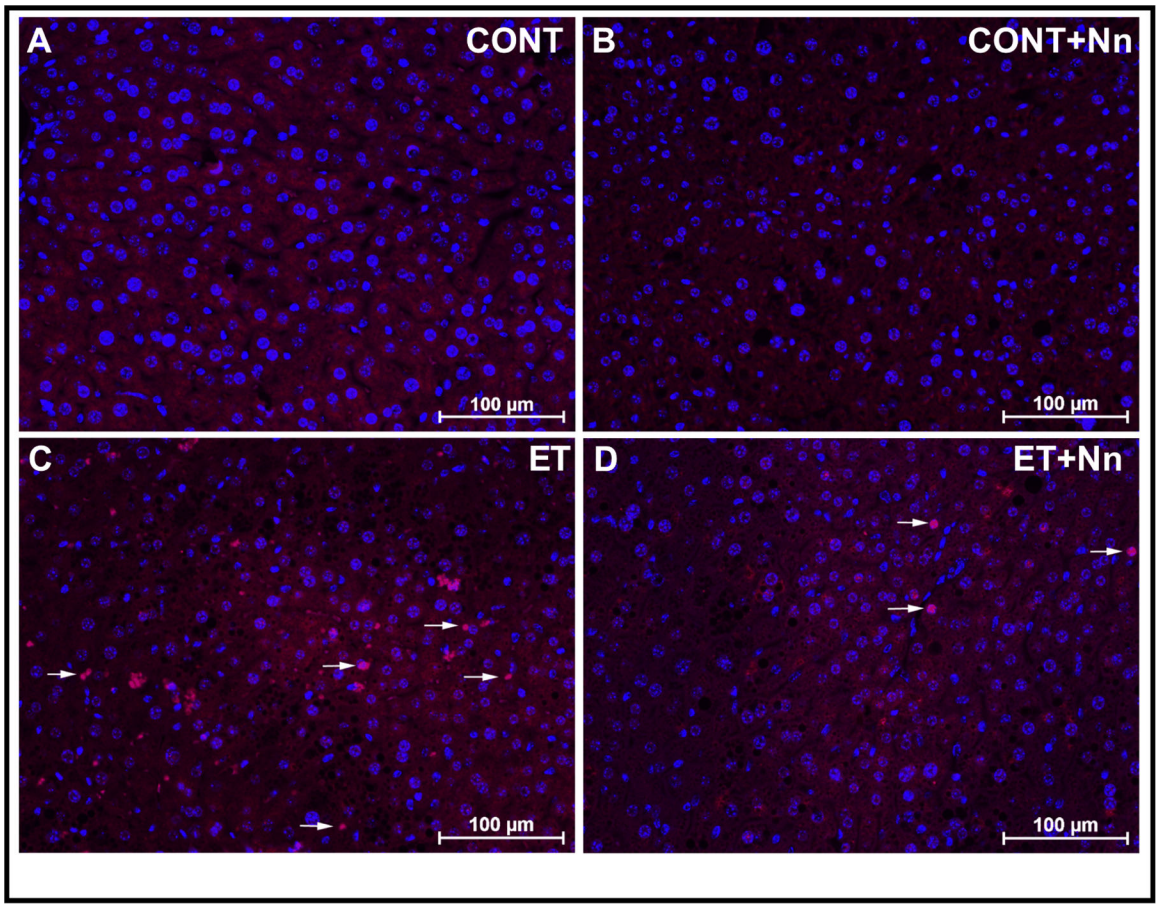

Fig. 6. Effect of Nano on the protein level of CCR2 in liver.

Liver sections (4µm) were stained for CCR2 protein by immunofluorescence method. Representative pictures taken at 20X magnification are shown (A-D).

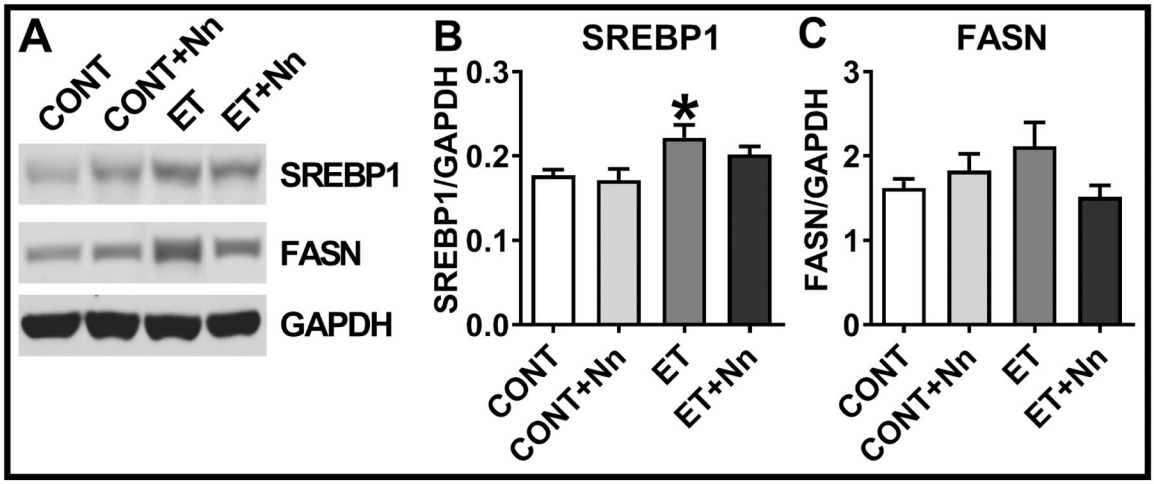

Fig. 7. Effect of Nano on markers of lipogenesis in liver.

Representative bands for proteins involved in lipogenesis are shown (A). Bands were quantified and values normalized to GAPDH. Protein levels of SREBP1 and FASN (B&C) are shown. Values are expressed as mean ± SEM of 6–8 samples in each group. **P*<0.05 vs CONT+Nn. CONT, control; ET, ethanol; Nn, Nano.

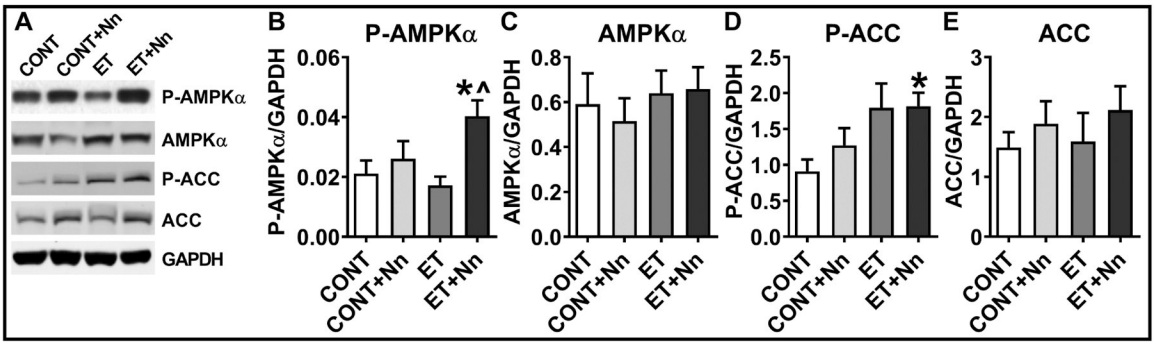

Fig. 8. Effect of Nano on AMPK signaling.

Liver homogenates were subjected to western blot analysis for markers of AMPK signaling. Representative bands from each group are shown (A). Bands were quantified and values normalized to GAPDH. Protein levels of phospho-AMPKα (P-AMPKα, B), total AMPKα (C), phospho-ACC (P-ACC, D), and total ACC (E) are shown. Values are expressed as mean ± SEM of 6–8 samples in each group. **P*<0.05 vs CONT; ^*P*<0.05 vs ET. CONT, control; ET, ethanol; Nn, Nano.

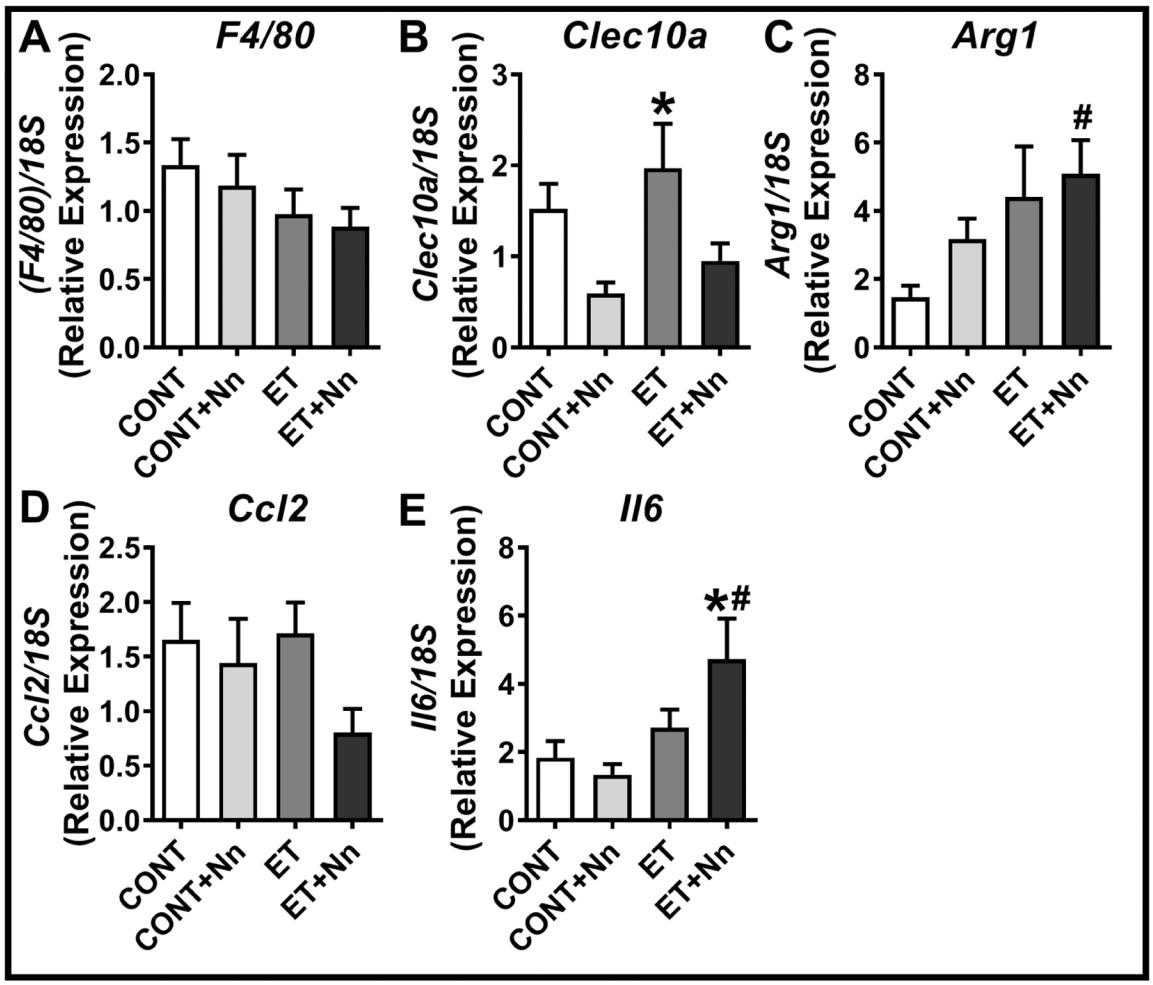

Fig. 9. Effect of Nano on AT inflammation.

Realtime PCR analysis was carried out in visceral AT samples for the mRNA levels of macrophages (A-C) and chemokine/cytokine (D&E). Values are normalized to 18S and expressed as mean ± SEM of 6–8 samples in each group. *$P<0.05$ vs CONT+Nn; $^{\#}P<0.05$ vs CONT. CONT, control; ET, ethanol; Nn, NanoSOD.